ACS SENSORS

Article

pubs.acs.org/acssensors

Nanoscale Thermal Management of Single SnO_2 Nanowire: pico-Joule Energy Consumed Molecule Sensor

Gang Meng,[†] Fuwei Zhuge,[†] Kazuki Nagashima,[†] Atsuo Nakao,[‡] Masaki Kanai,[†] Yong He,[†] Mickael Boudot,[†] Tsunaki Takahashi,[§] Ken Uchida,[§] and Takeshi Yanagida*[,†]

[†]Institute for Materials Chemistry and Engineering, Kyushu University, 6-1 Kasuga-Koen, Kasuga, Fukuoka 816-8580, Japan

[‡]Panasonic Corporation, 1006 Kadoma, Kadoma City, Osaka 571-8506, Japan

[§]Department of Electrical Engineering, Keio University, 3-14-1 Hiyoshi, Kouhokuku, Yokohama 223-8522, Japan

Supporting Information

ABSTRACT: Here we report the thermal management of oxide nanowire sensor in both spatial and time domains by utilizing unique thermal properties of nanowires, which are (1) the reduced thermal conductivity and (2) the short thermal relaxation time down to several microseconds. Our method utilizes a pulsed self-Joule-heating of suspended SnO_2 nanowire device, which enables not only the gigantic reduction of energy consumption down to $\sim 10^2$ pJ/s, but also enhancement of the sensitivity for electrical sensing of NO_2 (100 ppb). Furthermore, we demonstrate the applicability of the present method as sensors on flexible PEN substrate. Thus, this proposed thermal management concept of nanowires in both spatial and time domains offers a strategy for exploring novel functionalities of nanowire-based devices.

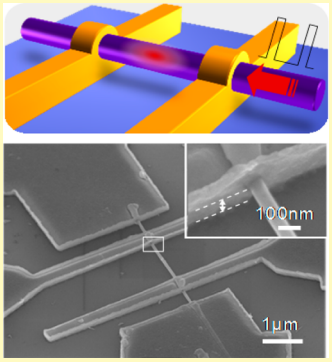

KEYWORDS: *nanoscale thermal management, single nanowire device, pulse measurement, thermal relaxation time, thermal conductivity, flexible device*

Electrical sensing of volatile molecular species in environments and/or from our bodies by using mobile electronics is an important issue for future electronic devices.[1,2] This is because these sensor electronics will have an impact on our daily life and healthcare via collecting and analyzing big data.[3] However, conventional gas sensors, including semiconductor oxide sensors, have been difficult to be integrated into CMOS electronics and wearable electronics due to the relatively high energy consumption (~J/s) to ensure a rapid and reversible sensing operation via programming the temperature of the sensor between ~470 and 670 K.[4−6] For example, most conventional metal oxide gas sensors are typically operated at the temperature ~510 K by using an external heater with 835 mJ/s.[7] The major reason that the conventional semiconductor gas sensors require relatively high energy consumption is that the external heater must heat up a large volume (typically $\sim 10^7$ μm^3) of sensors via solid heat conduction by competing with the heat dissipation into the surroundings.[7] Thus, thermal management is an important issue for designing sensor electronics.

Various concepts have been proposed to manage the thermal properties of sensors. Among them, microelectromechanical systems (MEMS) sensors with a microhotplate integrated on a Si_3N_4 membrane have recently emerged utilizing advanced lithographic technology.[8−17] The state-of-the-art membrane MEMS sensors have proven the feasibility to reduce the energy consumption down to ~20 mJ/s at 520 K via controlling the spatial temperature distribution on the membrane.[17] The fundamental design concepts include (1) to reduce the heat dissipation, (2) to decrease the sensor volume, and (3) to decrease the distance between the external heater and the sensing part. A suspended nanowire sensor with self-Joule-heating is an ideal sensing platform, which satisfies all the above requirements. This is because (1) the volume of the nanowire is extremely small ($\sim 10^{-3}$ μm^3), (2) the suspended nanowire structure substantially suppresses the heat dissipation into the surroundings, and (3) the self-Joule-heating method ultimately decreases the distance between the heater and the sensor. Comini et al. reported their pioneering work of nanowire gas sensors using SnO_2 nanobelts, which was a nonsuspended device without self-Joule-heating.[18] Prades et al.[19,20] have demonstrated the reduction of energy consumption down to 20 μJ/s using self-Joule-heating in nonsuspended SnO_2 nanowire sensors. However, there seems to be a fundamental limitation to further enhancing the sensing characteristics, including the energy consumption and the sensitivity, even using these nanowire sensors.[21−23] One of major reasons these previous studies of nanowire sensors have failed to further tailor the sensing properties seems to be that they have focused on

Received: June 2, 2016
Accepted: July 4, 2016
Published: July 4, 2016

DOI: 10.1021/acssensors.6b00364
ACS Sens. 2016, 1, 997−1002

only controlling the spatial thermal properties of nanowires.[19−23]

Here we propose the thermal management of oxide nanowire sensors in both spatial and time domains, which enables not only the reduction of energy consumption of volatile molecule sensors down to ~10^2 pJ/s, but also the sensitivity higher than conventional continuous heating method. Our method focuses on the short thermal relaxation time (~μs) of suspended SnO_2 nanowire device, which is defined as the time required for heating up/or cooling down to a desired temperature. The thermal relaxation time of the nanowire device is much shorter than other existing semiconductor gas sensors mainly due to the smaller volume of nanowire sensors and characteristics of self-Joule-heating. Since the energy consumption of sensors depends on not only the heating power but also the heating time, this short thermal relaxation time of nanowire sensors essentially allows us to reduce the energy consumption of sensors by heating up only during sensing using a pulse mode. In addition, the reduced thermal conductivity of nanowires plays an important role in the spatial thermal management of nanowire sensors for increasing local temperature via self-Joule heating. Thus, the present methodology based on the thermal management of nanowire sensors in both spatial and time domains offers a new strategy to tailor the properties of nanowire-based devices.

EXPERIMENTAL SECTION

SnO_2 Nanowire Growth. Single-crystalline SnO_2 nanowires were synthesized by pulsed laser deposition (PLD) method, as described in previous work.[24,25] Al_2O_3(110) substrate with Au layer of 0.7 nm was heated up to 750 °C under O_2 and Ar mixed gas (O_2:Ar = 1:1000, total pressure of 10 Pa). SnO_2 target (purity 99.99%) was ablated by ArF excimer laser (wavelength of 193 nm, energy of 40 mJ, and repetition of 10 Hz). By carefully controlling supplied metal and O_2 flux, SnO_2 nanowires were obtained via a vapor−liquid−solid (VLS) process. Fabricated nanowires were characterized by field emission scanning electron microscope (FESEM), X-ray diffraction (XRD), and high-resolution transmission electron microscope (HRTEM). The detailed results can be seen in the SI Figure S1.

Device Fabrication. SnO_2 nanowire sensor devices were fabricated by conventional lithography techniques using electron beam lithography (EBL) and radiofrequency (RF) sputtering.[25,26] As-grown SnO_2 nanowires were deposited onto SiO_2/Si (100) substrate with predefined Ti/Pt metal electrodes. Then EBL was employed to define contact electrodes. After Ti/Au layer (1 nm Ti/300 nm Au) deposition and lift-off process, conventional nonsuspended devices could be obtained. For the case of suspended devices, an MgO sacrifice layer with thickness of 100 nm was deposited onto the SiO_2/Si or polyethylene naphthalate (PEN) substrates to create an air-gap between nanowire and substrate. After the EBL and electrode deposition processes, the MgO sacrifice layer was removed by a dilute HCl solution (12 mM), resulting in a suspended nanowire device. It should be noted that the suspended nanowires were susceptible to attachment to the substrate in the final drying process, owing to a strong meniscus force.[27,28] To avoid this problem, instead of distilled water (surface tension of 72.8 mN/m at 20 °C), low surface tension solvent, such as ethanol (22.1 mN/m at 20 °C) or hydrofluoroether (HFE, 13.6 mN/m at 20 °C), was utilized in the final rinsing and drying process. More detailed procedures can be found in SI Figure S2.

Electrical Measurements. Thermal relaxation time of suspended SnO_2 nanowires and NO_2 response experiments were measured by semiconductor parameter analyzer (Keithley 4200 SCS), connected with a probe station in which ambient pressure and stage temperature can be controlled. To estimate the thermal relaxation time, the SnO_2 nanowire devices were initially evacuated to a base pressure of 2 × 10^{-2} Pa.[29] Keithley pulse module (PMU 4225) was employed to measure the short transition time from low voltage (room temperature T_0) to high voltage (equilibrium temperature T_{equiv}). Sampling rate was set to be 10 MHz; a spot mean measurement of 10 points ensures monitoring resistance variation with the time resolution of 1 μs. NO_2 response was also carried out by operating under both self-Joule-heating and external heating (RT - 523 K) mode. Resistance of the SnO_2 nanowire under vacuum was recorded as baseline (R_0). The resistance upon exposure of NO_2 gas with an equivalent concentration of 100 ppb (by injecting 100 ppm of NO_2 into the chamber to be 100 Pa) was noted as R. Finally, the chamber was re-evacuated for recovery. Sensitivity was defined as R/R_0 × 100%.

Simulation. Numerical simulation (COMSOL Multiphysics) was performed to examine the nanoscale thermal transport of suspended nanowire devices. In order to achieve a reliable simulation, several important physical parameters, such as electrical conductivity (σ), temperature dependence of resistivity, and thermal conductivity (κ) of SnO_2 nanowires, were experimentally extracted by 4-probe, temperature dependent 4-probe, and 3-omega (3ω) method, respectively. Additional information on simulation can be seen in SI Figure S3−S8.

RESULTS AND DISCUSSION

First, we numerically examine the effect of self-Joule-heating on the temperature distribution of suspended nanowire devices, in order to obtain the spatial thermal information. The schematic model is illustrated in Figure 1a, and the details of numerical

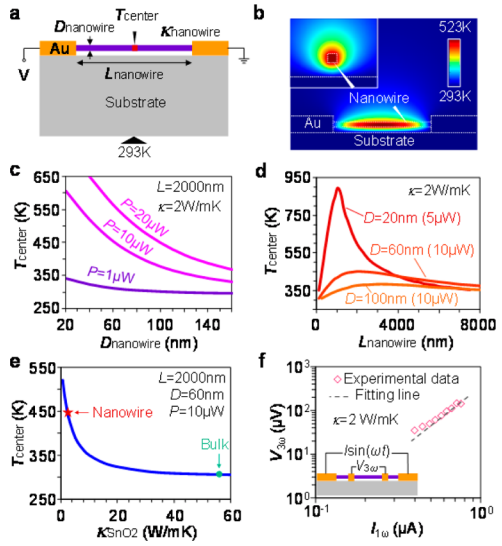

Figure 1. Simulated thermal properties for self-Joule-heating of nanowire device. (a) Schematic model for numerical simulation. (b) Temperature distribution of self-Joule-heating nanowire device. Inset shows the cross-sectional temperature distribution at the nanowire center. (c) Effect of nanowire diameter on temperature at the nanowire center, T_{center}, when varying the Joule heat power. (d) Effect of nanowire length on temperature at the nanowire center, T_{center}, when varying the Joule heat power. (e) Effect of thermal conductivity of the nanowire on temperature at the nanowire center, T_{center}, under fixed Joule heat power of 10 μW. (f) Thermal conductivity measurement of the present SnO_2 nanowires by the 3 omega method.

simulation can be seen in SI Figure S3. The temperature at the center of the nanowire (T_{center}) was highest due to the heat dissipation into electrodes,[30] as shown in Figure 1b. We utilize this temperature value at the center of nanowire to quantitatively examine the effects of various device parameters, including the values of length ($L_{nanowire}$), diameter ($D_{nanowire}$), and thermal conductivity of nanowires ($\kappa_{nanowire}$), on the Joule heating under a fixed input power. Figure 1c−e shows the

DOI: 10.1021/acssensors.6b00364
ACS Sens. 2016, 1, 997−1002

simulation results. We found that several device properties can significantly lower the input power for Joule heating of the suspended nanowire devices. The smaller diameter of nanowires lowers the necessary input power to reach the equilibrium temperature via Joule heating due to the smaller volume, as shown in Figure 1c. However, decreasing the volume via decreasing the nanowire length did not result in the suppression of input power due to the significant heat dissipation into electrodes.[31] Thus, there was an optimal length of nanowires for effective self-Joule-heating, as shown in Figure 1d. This is due to the competition between the heat dissipation into electrodes and the heat dissipation into surrounding air. Therefore, (i) the small volume of nanowires and (ii) the optimal device configuration to minimize the heat dissipation into surroundings are important characteristics to lower the input power for Joule heating in the suspended nanowire devices. One more important parameter is the thermal conductivity of nanowires, which critically determines the heat dissipation into surroundings though nanowire/electrode and nanowire/surrounding-gas interfaces, as shown in Figure 1e. We measured the thermal conductivity of the present SnO_2 nanowires via the 3ω method,[32] as shown in Figure 1f. The thermal conductivity of the present [100] orientated SnO_2 nanowires was 2 W/mK (diameter of 79 nm), which is about 27 times lower than that of bulk single crystalline SnO_2 (perpendicular to c-axis 55 W/mK).[33] This lowered thermal conductivity of nanowires[34] significantly suppresses Joule heat dissipation into the surroundings, resulting in the efficient temperature increase within the confined spatial position of the nanowire.[35]

Next, we focus on the thermal relaxation time τ, which is defined as a characteristic time during heating up or cooling down.[36] This is an important parameter for thermal management in a time domain. We have performed both experiments and simulations to extract the thermal relaxation time of the suspended nanowire device. Figure 2a shows the SEM image of suspended nanowire devices utilizing single crystalline SnO_2 nanowires grown by a vapor−liquid−solid (VLS) method.[24,25] As designed, SnO_2 nanowire was fully suspended between electrodes and SiO_2/Si substrate. The details of the fabrication processes of the suspended nanowire devices can be seen in SI Figure S2. In order to estimate the actual thermal relaxation time of the suspended nanowire device, first we measured the temperature dependence of nanowire resistivity by the 4-probe method; the temperature is programmed by an external heater, as shown in Figure 2b. Elevating the temperature results in the decrease of resistivity, revealing the semiconducting behavior of SnO_2 nanowires with the activation energy of 79.9 meV.[37] Next, we performed ultrafast current−voltage (IV) measurement to experimentally extract the thermal relaxation time. Figure 2c shows the waveform of pulse voltage V, the resistivity ρ, and estimated temperature of suspended nanowire device T_{equiv}. It can be seen that the resistivity change occurs within a microsecond, which is the time resolution of our experimental systems. The elevated temperature value of the nanowire was estimated to be ∼520 K from the temperature dependence data in Figure 2b. To validate the thermal relaxation time in simulations, the time series data of T_{center} when performing self-Joule-heating have been calculated. As shown in the gray line in Figure 2c, there is good agreement between experimental data and the simulated values. In most device configurations employed in our experiments, the thermal relaxation times were found to be in a microsecond range. Thus, these results highlight that the short thermal relaxation time of nanowire devices allows us to manage the temperature time profile in the range of microseconds. Since the thermal relaxation times of conventional gas sensors and recent MEMS gas sensors are several tens of seconds and several tens of milliseconds,[13,15,38,39] respectively, our method utilizing the microsecond thermal relaxation time of nanowire devices enables us to further tailor the thermal properties in time domains beyond the limitation of conventional methodologies.

We examine the feasibility of our thermally managed nanowire devices for volatile molecule sensors. The device configuration ($L_{nanowire}$ = 1850 nm, $D_{nanowire}$ = 57 nm) is designed based on numerical study in Figure 1. NO_2 gas (100 ppb) was employed for the present sensing experiments. Figure 3 shows the comparison between different heating methods,

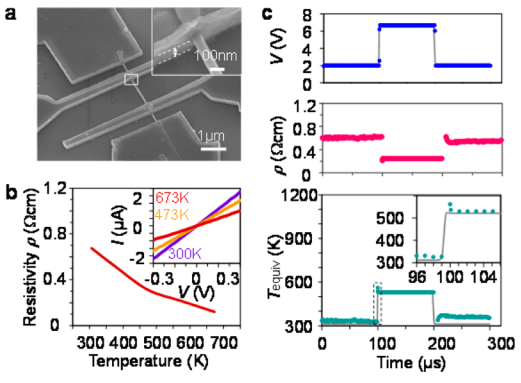

Figure 2. Evaluation of thermal relaxation time. (a) SEM image of suspended 4-terminal SnO_2 nanowire device. (b) Temperature dependence of electrical resistivity of fabricated suspended SnO_2 nanowire device. Inset shows the current−voltage (IV) curves for various temperatures. (c) Time series data of applied voltage, measured resistivity, and estimated temperatures during ultrafast IV measurement, shown by dots. Time dependent simulation results have been shown by gray lines. Both experiment and simulation reveal the short thermal relaxation time of ∼μs.

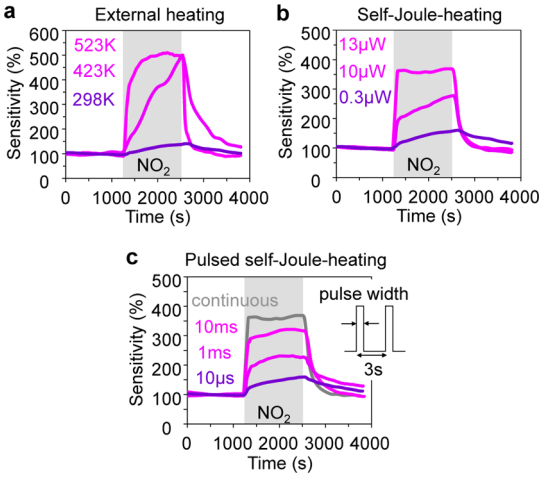

Figure 3. Sensing data of suspended nanowire device when introducing NO_2 (100 ppb). (a) Sensing data of external heating mode using an external heater. (b) Sensing data of continuous self-Joule-heating mode. (c) Sensing data of pulsed self-Joule-heating mode, measured under a constant Joule power of 13 μW (during pulse on).

DOI: 10.1021/acssensors.6b00364
ACS Sens. 2016, 1, 997−1002

including (a) external heating, (b) self-Joule-heating, and (c) pulsed self-Joule-heating, on the resistance change of suspended nanowire devices when introducing NO_2 gas (100 ppb). For all heating systems, introducing NO_2 gas increased the resistance of SnO_2 nanowire, as reported elsewhere.[18,19] In external heating system, increasing the temperature from 300 to 520 K significantly enhanced the sensitivity via promoting the chemisorption on the oxide surface.[4] A similar trend on the sensitivity was also observed when increasing the current value for the self-Joule-heating system. For the pulsed self-Joule-heating system, there pulse width was dependent on the sensitivity. Increasing the pulse width enhanced the sensitivity. However, the sensitivity change was not significant when considering the fact that the pulse width decreased down to less than 1/100. For example, in the case of the pulse width (1 ms), the sensitivity was almost 60% of the continuous heating data, although the nanowire was heated up during just 0.03% of total time. Thus, the present results highlight that the suspended nanowire sensor does not require the continuous heating condition for the electrical sensing. Table 1 shows the

Table 1. Comparison between Three Methods (External Heating, Self-Joule-Heating, and Pulsed Self-Joule-Heating) on the Energy Consumption to Reach the Sensitivity of 200% for NO_2 (100 ppb)

	external heating	self-Joule-heating	pulsed self-Joule-heating
energy consumption	0.6 J/s	1.6 μJ/s	0.6 nJ/s

comparison between the three heating methods on the consumed energy value to reach the sensitivity of 200%. As clearly seen, the present pulsed self-Joule-heating method in suspended nanowire device can lower the energy consumption down to 0.6 nJ/s (adjusting the pulse width to be 140 μs for a Joule power of 13 μW), which is much lower than the other two methods. The substantial reduction of energy consumption can be ascribed to the thermal management of suspended nanowire in both spatial and time domains based on the unique thermal properties of nanowires, such as the low thermal conductivity[34,35] and the short thermal relaxation time. Suspended nanowire can be heated up to a higher temperature within a short electrical pulse to activate the charge exchange between absorbed molecules and nanowire surface even without continuous heating.[40] Thus, the thermal management in both spatial and time domains substantially reduces the energy consumption of the nanowire sensor.

Next, we question why the thermally managed nanowire sensor using a pulse heating exhibited relatively good sensitivity in spite of the fact that the cumulative heating time for pulse heating is less than 1% of the continuous heating method. To answer this, we have performed transient measurements when applying a pulse heating, as shown in Figure 4a. As can be seen, the resistance increased when the nanowire was heated up during the pulse. The modulated resistance change was maintained until the next pulse heating. This indicates that the molecules chemisorbed onto the nanowire surface might be frozen between two pulses at lower temperature, as illustrated in Figure 4b. This can be understood by considering the fact that an energy barrier exists for desorption from the chemisorbed state.[41] These "frozen" chemisorbed molecules on the nanowire surface are mainly responsible for the relatively high sensitivity of the pulse heating method. However, even for

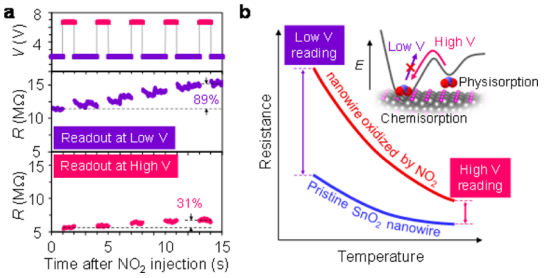

Figure 4. Enhanced sensitivity of pulse measurement and the underlying mechanism. (a) Transient response of the suspended SnO_2 nanowire device for sensing NO_2 (100 ppb). Resistance values read at high voltage (red dots) and low voltage (purple dots) after NO_2 injection are shown. (b) Mechanism to explain the enhancement of sensitivity of pulse measurement when reading the resistance value at lower temperature during pulse-off. The difference between two TCR curves of pristine SnO_2 nanowire (blue line) and SnO_2 nanowire oxidized by NO_2 molecules (red line) can explain the observed enhancement of sensitivity of pulse measurements.

constant cumulative heating time, there is a difference between the pulse heating method and the continuous heating method on the sensitivity. Although it is difficult to obtain the direct experimental evidence, it is considered that the physisorption of molecules was promoted at lower temperatures during cooling time,[4,41] which increases the molecular concentration near the nanowire surface for chemisorption of molecules during pulse heating. The other interesting feature of the thermal management in both spatial and time domains is the enhancement of sensitivity via reading the electrical resistance at lower temperature during pulses. As shown in Figure 4, the sensitivity was significantly enhanced when decreasing the reading voltage between pulse heating. This sensitivity enhancement can be interpreted in terms of different temperature coefficient of resistance (TCR),[42,4] as illustrated in Figure 4b. In principle, the temperature dependence of semiconductors tends to be stronger as carrier concentration decreases. When oxidizing for n-type SnO_2 nanowires by NO_2, the carrier concentration of SnO_2 nanowires decreases. Thus, the sensitivity, defined as the resistance ratio of the pristine SnO_2 nanowire to SnO_2 nanowire oxidized by NO_2, can be enhanced by reading the resistance values at the lower temperature, as illustrated. To the best of our knowledge, such a sensitivity enhancement concept has not been reported, probably due to relatively long thermal relaxation time of external heating for other existing sensors.[13,15,38,39] Thus, the thermal management in both spatial and time domains significantly enhances the sensing properties.

Finally, we demonstrate the feasibility of the present pulsed heating method for wearable sensors, which can be conveniently attached onto human skin or plants.[43] We have fabricated suspended SnO_2 nanowires on the flexible PEN substrate. Figure 5a shows the device on PEN substrate. Metal oxide gas sensors, which require high temperature operation, have been difficult to integrate into such polymers with relatively low glass transition temperatures.[44] As shown in Figure 5b, conventional external heating up to 523 K damaged the PEN substrate. On the other hand, the pulsed heating method can be performed without any damage to the PEN substrate. Figure 5c shows the NO_2 sensing data of the SnO_2 nanowire sensor devices on PEN substrate, under the pulsed self-heating mode, with pulse width of 10 μs and period of 3 s. Thus, the present methodology offers tremendous opportunities for wearable sensors on flexible sensors.

DOI: 10.1021/acssensors.6b00364
ACS Sens. 2016, 1, 997−1002

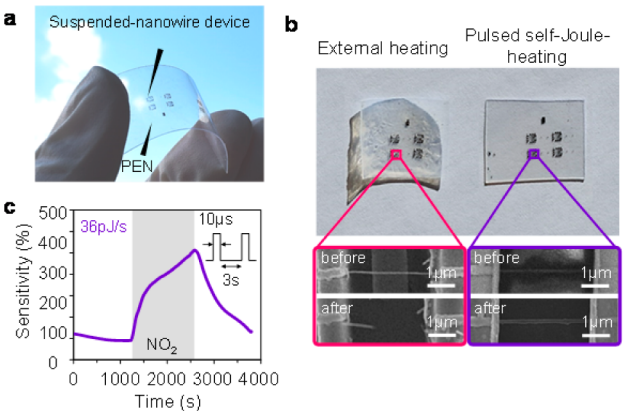

Figure 5. Applications of the present methodology to flexible substrate. (a) Photograph of suspended SnO_2 nanowire device formed on the flexible PEN substrate. (b) Photographs of PEN devices operated under external heating (left) and pulsed self-Joule-heating (right). SEM images of nanowire device taken before and after sensing experiments are shown at the bottom. (c) Sensing data of suspended SnO_2 nanowire device on PEN substrate to 100 ppb NO_2 molecules.

CONCLUSIONS

In summary, we demonstrated the impact of thermal management of oxide nanowire sensors on the sensing characteristics. The thermal management of nanowires was performed in both spatial and time domains by utilizing the unique thermal properties of nanowires, which are (1) the reduced thermal conductivity and (2) the short thermal relaxation time down to several microseconds. This method enables not only the reduction of energy consumption down to ~10^2 pJ/s, but also the enhancement of sensitivity for electrical sensing of NO_2 (100 ppb). Furthermore, we demonstrate the applicability of the present methodology as gas sensors on flexible substrates.

ASSOCIATED CONTENT

Supporting Information

The Supporting Information is available free of charge on the ACS Publications website at DOI: 10.1021/acssensors.6b00364.

Nanowire properties and procedures to fabricate suspended device; analysis of self-Joule-heating in nanowire device; continuous operation of self-heated SnO_2 nanowire sensor (PDF)

AUTHOR INFORMATION

Corresponding Author

*E-mail: yanagida@cm.kyushu-u.ac.jp.

Notes

The authors declare no competing financial interest.

ACKNOWLEDGMENTS

This work was supported by CREST of Japan Science and Technology Corporation (JST). This work was performed under the Cooperative Research Program of "Network Joint Research Center for Materials and Devices". We thank Dr. Yuhui He and Dr. Keju Sun for fruitful discussions.

REFERENCES

(1) Shehada, N.; Bronstrup, G.; Funka, K.; Christiansen, S.; Leja, M.; Haick, H. Ultrasensitive Silicon Nanowire for Real-World Gas Sensing: Noninvasive Diagnosis of Cancer from Breath Volatolome. *Nano Lett.* **2015**, *15*, 1288−1295.

(2) Comini, E. Metal oxide nano-crystals for gas sensing. *Anal. Chim. Acta* **2006**, *568*, 28−40.

(3) Duran-Frigola, M.; Rossell, D.; Aloy, P. A chemo-centric view of human health and disease. *Nat. Commun.* **2014**, *5*, 5676.

(4) Gurlo, A. Interplay between O_2 and SnO_2: Oxygen ionosorption and spectroscopic evidence for adsorbed oxygen. *ChemPhysChem* **2006**, *7*, 2041−2052.

(5) Wang, C. X.; Yin, L. W.; Zhang, L. Y.; Xiang, D.; Gao, R. Metal Oxide Gas Sensors: Sensitivity and Influencing Factors. *Sensors* **2010**, *10*, 2088−2106.

(6) *Semiconductor gas sensors*; Woodhead Publishing Limited: Cambridge, 2013.

(7) *TGS816*; http://www.figaro.co.jp/en/product/entry/tgs816.html (accessed September 24, 2015).

(8) Pike, A.; Gardner, J. W. Thermal modelling and characterisation of micropower chemoresistive silicon sensors. *Sens. Actuators, B* **1997**, *45*, 19−26.

(9) Rossi, C.; Temple-Boyer, P.; Esteve, D. Realization and performance of thin SiO_2/SiN_x membrane for microheater applications. *Sens. Actuators, A* **1998**, *64*, 241−245.

(10) Sheng, L. Y.; Tang, Z. N.; Wu, J.; Chan, P. C. H.; Sin, J. K. O. A low-power CMOS compatible integrated gas sensor using maskless tin oxide sputtering. *Sens. Actuators, B* **1998**, *49*, 81−87.

(11) Solzbacher, F.; Imawan, C.; Steffes, H.; Obermeier, E.; Moeller, H. A modular system of SiC-based microhotplates for the application in metal oxide gas sensors. *Sens. Actuators, B* **2000**, *64*, 95−101.

(12) Solzbacher, F.; Imawan, C.; Steffes, H.; Obermeier, E.; Eickhoff, M. A new SiC/HfB_2 based low power gas sensor. *Sens. Actuators, B* **2001**, *77*, 111−115.

(13) Afridi, M. Y.; Suehle, J. S.; Zaghloul, M. E.; Berning, D. W.; Hefner, A. R.; Cavicchi, R. E.; Semancik, S.; Montgomery, C. B.; Taylor, C. J. A Monolithic CMOS Microhotplate-Based Gas Sensor System. *IEEE Sens. J.* **2002**, *2*, 644−655.

(14) Briand, D.; Heimgartner, S.; Gretillat, M. A.; van der Schoot, B.; de Rooij, N. F. Thermal optimization of micro-hotplates that have a silicon island. *J. Micromech. Microeng.* **2002**, *12*, 971−978.

(15) Mo, Y. W.; Okawa, Y. Z.; Inoue, K. J.; Natukawa, K. Low-voltage and low-power optimization of micro-heater and its on-chip drive circuitry for gas sensor array. *Sens. Actuators, A* **2002**, *100*, 94−101.

(16) Guha, P.; Ali, S.; Lee, C.; Udrea, F.; Milne, W.; Iwaki, T.; Covington, J.; Gardner, J. Novel design and characterisation of SOI CMOS micro-hotplates for high temperature gas sensors. *Sens. Actuators, B* **2007**, *127*, 260−266.

(17) Dai, Z.; Xu, L.; Duan, G.; Li, T.; Zhang, H.; Li, Y.; Wang, Y.; Wang, Y.; Cai, W. Fast-Response, Sensitivitive and Low-Powered Chemosensors by Fusing Nanostructured Porous Thin Film and IDEs-Microheater Chip. *Sci. Rep.* **2013**, *3*, 1669.

(18) Comini, E.; Faglia, G.; Sberveglieri, G.; Pan, Z. W.; Wang, Z. L. Stable and highly sensitive gas sensors based on semiconducting oxide nanobelts. *Appl. Phys. Lett.* **2002**, *81*, 1869−1871.

(19) Prades, J. D.; Jimenez-Diaz, R.; Hernandez-Ramirez, F.; Barth, S.; Cirera, A.; Romano-Rodriguez, A.; Mathur, S.; Morante, J. R. Ultralow power consumption gas sensors based on self-heated individual nanowires. *Appl. Phys. Lett.* **2008**, *93*, 123110.

(20) Prades, J. D.; Jimenez-Diaz, R.; Hernandez-Ramirez, F.; Pan, J.; Romano-Rodriguez, A.; Mathur, S.; Morante, J. R. Direct observation of the gas-surface interaction kinetics in nanowires through pulsed self-heating assisted conductometric measurements. *Appl. Phys. Lett.* **2009**, *95*, 053101.

(21) Chikkadi, K.; Muoth, M.; Maiwald, V.; Roman, C.; Hierold, C. Ultra-low power operation of self-heated, suspended carbon nanotube gas sensors. *Appl. Phys. Lett.* **2013**, *103*, 223109.

DOI: 10.1021/acssensors.6b00364
ACS Sens. 2016, 1, 997−1002

(22) Meier, D. C.; Semancik, S.; Button, B.; Strelcov, E.; Kolmakov, A. Coupling nanowire chemiresistors with MEMS microhotplate gas sensing platforms. *Appl. Phys. Lett.* **2007**, *91*, 063118.
(23) Yun, J.; Jin, C. Y.; Ahn, J. H.; Jeon, S.; Park, I. A self-heated silicon nanowire array: selective surface modification with catalytic nanoparticles by nanoscale Joule heating and its gas sensing applications. *Nanoscale* **2013**, *5*, 6851−6856.
(24) Klamchuen, A.; Yanagida, T.; Kanai, M.; Nagashima, K.; Oka, K.; Kawai, T.; Suzuki, M.; Hidaka, Y.; Kai, S. Role of surrounding oxygen on oxide nanowire growth. *Appl. Phys. Lett.* **2010**, *97*, 073114.
(25) Meng, G.; Yanagida, T.; Nagashima, K.; Yoshida, H.; Kanai, M.; Klamchuen, A.; Zhuge, F. W.; He, Y.; Rahong, S.; Fang, X. D.; Takeda, S.; Kawai, T. Impact of Preferential Indium Nucleation on Electrical Conductivity of Vapor-Liquid-Solid Grown Indium-Tin Oxide Nanowires. *J. Am. Chem. Soc.* **2013**, *135*, 7033−7038.
(26) Nagashima, K.; Yanagida, T.; Oka, K.; Kanai, M.; Klamchuen, A.; Rahong, S.; Meng, G.; Horprathum, M.; Xu, B.; Zhuge, F.; He, Y.; Park, B. H.; Kawai, T. Prominent Thermodynamical Interaction with Surroundings on Nanoscale Memristive Switching of Metal Oxides. *Nano Lett.* **2012**, *12*, 5684−5890.
(27) Zhang, C. Y.; Zhang, X. J.; Zhang, X. H.; Fan, X.; Jie, J. S.; Chang, J. C.; Lee, C. S.; Zhang, W. J.; Lee, S. T. Heat dissipation from suspended self-heated nanowires: gas sensor prospective. *Adv. Mater.* **2008**, *20*, 1716−1270.
(28) He, Y.; Nagashima, K.; Kanai, M.; Meng, G.; Zhuge, F.; Rahong, S.; Li, X.; Kawai, T.; Yanagida, T. Nanoscale Size-Selective Deposition of Nanowires by Micrometer Scale Hydrophilic Patterns. *Sci. Rep.* **2014**, *4*, 5943.
(29) Nanayakkara, C. E.; Larish, W. A.; Grassian, V. H. Titanium Dioxide Nanoparticle Surface Reactivity with Atmospheric Gases, CO_2, SO_2, and NO_2: Roles of Surface Hydroxyl Groups and Adsorbed Water in the Formation and Stability of Adsorbed Products. *J. Phys. Chem. C* **2014**, *118*, 23011−23021.
(30) Xu, T. T.; Wei, X. L.; Shu, J. P.; Chen, Q. Transmission electron microscopy assisted in-situ joule heat dissipation study of individual InAs nanowires. *Appl. Phys. Lett.* **2013**, *103*, 193112.
(31) Zhang, J.; Strelcov, E.; Kolmakov, A. Heat dissipation from suspended self-heated nanowires: gas sensor prospective. *Nanotechnology* **2013**, *24*, 444009.
(32) Lu, L.; Yi, W.; Zhang, D. L. 3 omega method for specific heat and thermal conductivity measurements. *Rev. Sci. Instrum.* **2001**, *72*, 2996−3003.
(33) Turkes, P.; Pluntke, C.; Helbig, R. Thermal-Conductivity of Sno_2 Single-Crystals. *J. Phys. C: Solid State Phys.* **1980**, *13*, 4941−4951.
(34) Li, D. Y.; Wu, Y. Y.; Kim, P.; Shi, L.; Yang, P. D. Thermal conductivity of individual silicon nanowires. *Appl. Phys. Lett.* **2003**, *83*, 2934−2936.
(35) Kim, Y. D.; Kim, H.; Cho, Y.; Ryoo, J. H.; Park, C. H.; Kim, P.; Kim, Y. S.; Lee, S.; Li, Y. L.; Park, S. N.; Yoo, Y. S.; Yoon, D.; Dorgan, V. E.; Pop, E.; Heinz, T. F.; Hone, J.; Chun, S. H.; Cheong, H.; Lee, S. W.; Bae, M. H.; Park, Y. D. Bright visible light emission from graphene. *Nat. Nanotechnol.* **2015**, *10*, 676−681.
(36) Graf, M.; Barrettino, D.; Kirstein, K. U.; Hierlemann, A. CMOS microhotplate sensor system for operating temperatures up to 500 degrees C. *Sens. Actuators, B* **2006**, *117*, 346−352.
(37) Kolmakov, A.; Zhang, Y. X.; Cheng, G. S.; Moskovits, M. Detection of CO and O_2 using tin oxide nanowire sensors. *Adv. Mater.* **2003**, *15*, 997−1000.
(38) Semancik, S.; Cavicchi, R. Kinetically controlled chemical sensing using micromachined structures. *Acc. Chem. Res.* **1998**, *31*, 279−287.
(39) Suehle, J. S.; Cavicchi, R. E.; Gaitan, M.; Semancik, S. Tin oxide gas sensor fabricated using CMOS micro-hotplates and in-situ processing. *IEEE Electron Device Lett.* **1993**, *14*, 118−120.
(40) Moon, H. G.; Shim, Y. S.; Kim, D. H.; Jeong, H. Y.; Jeong, M.; Jung, J. Y.; Han, S. M.; Kim, J. K.; Kim, J. S.; Park, H. H.; Lee, J. H.; Tuller, H. L.; Yoon, S. J.; Jang, H. W. *Sci. Rep.* **2012**, *2*, 588.
(41) Hudson, J. B. *Surface science: an introduction*; Butterworth-Heinemann: Boston, 1992.
(42) Jarzebski, Z. M. Physical Properties of SnO_2 Materials. *J. Electrochem. Soc.* **1976**, *123*, 299C.
(43) Lee, K.; Park, J.; Lee, M.-S.; Kim, J.; Hyun, B. G.; Kang, D. J.; Na, K.; Lee, C. Y.; Bien, F.; Park, J.-U. In-situ Synthesis of Carbon Nanotube-Graphite Electronic Devices and Their Integrations onto Surfaces of Live Plants and Insects. *Nano Lett.* **2014**, *14*, 2647−2654.
(44) Oprea, A.; Barsan, N.; Weimar, U.; Courbat, J.; Briand, D.; de Rooij, N. F. Integrated Temperature, Humidity and Gas Sensors on Flexible Substrates for Low-Power Applications. *IEEE Sensor* **2007**, 158−161.

DOI: 10.1021/acssensors.6b00364
ACS Sens. 2016, 1, 997−1002